

Article

Wearable Natural Rubber Latex Gloves with Curcumin for Torn Glove Detection in Clinical Settings

Norfatirah Muhamad Sarih ¹, Nuur Syuhada Dzulkafly ¹, Simon Maher ² and Azura A. Rashid ^{1,*} 

¹ School of Materials and Mineral Resources Engineering, Universiti Sains Malaysia, Engineering Campus, Nibong Tebal 14300, Penang, Malaysia; fatirahsarih@usm.my (N.M.S.); dn.syuhada@student.usm.my (N.S.D.)

² Department of Electrical Engineering and Electronics, University of Liverpool, Liverpool L69 3GJ, UK; s.maher@liverpool.ac.uk

* Correspondence: srazura@usm.my

Abstract: Glove tear or perforation is a common occurrence during various activities that require gloves to be worn, posing a significant risk to the wearer and possibly others. This is vitally important in a clinical environment and particularly during surgical procedures. When a glove perforation occurs (and is noticed), the glove must be replaced as soon as possible; however, it is not always noticeable. The present article is focused on the design and development of a novel fluorescence-based sensing mechanism, which is integrated within the glove topology, to help alert the wearer of a perforation in situ. We hypothesized that natural rubber gloves with curcumin infused would yield fluorescence when the glove is damaged, particularly when torn or punctured. The glove design is based on double-dipping between Natural Rubber Latex (NRL) and an inner layer of latex mixed with curcumin, which results in a notable bright yellow-green emission when exposed to UV light. Curcumin (Cur) is a phenolic chemical found primarily in turmeric that fluoresces yellowish-green at 525 nm. The tear region on the glove will glow, indicating the presence of a Cur coating/dipping layer beneath. NRL film is modified by dipping it in a Cur dispersion solution mixed with NRL for the second dipping layer. Using Cur as a filler in NRL also has the distinct advantage of allowing the glove to be made stronger by evenly distributing it throughout the rubber phase. Herein, the optimized design is fully characterized, including physicochemical (fluorescence emission) and mechanical (tensile and tear tests) properties, highlighting the clear potential of this novel and low-cost approach for in situ torn glove detection.

Keywords: natural rubber latex; curcumin; fluorescence-based sensor; torn glove detection; wearable sensor; surgical gloves



Citation: Sarih, N.M.; Dzulkafly, N.S.; Maher, S.; Rashid, A.A. Wearable Natural Rubber Latex Gloves with Curcumin for Torn Glove Detection in Clinical Settings. *Polymers* **2022**, *14*, 3048. <https://doi.org/10.3390/polym14153048>

Academic Editor: Emin Bayraktar

Received: 6 July 2022

Accepted: 26 July 2022

Published: 28 July 2022

Publisher's Note: MDPI stays neutral with regard to jurisdictional claims in published maps and institutional affiliations.



Copyright: © 2022 by the authors. Licensee MDPI, Basel, Switzerland. This article is an open access article distributed under the terms and conditions of the Creative Commons Attribution (CC BY) license (<https://creativecommons.org/licenses/by/4.0/>).

1. Introduction

Surgical gloves act as a physical barrier between the surgeon's hands and the patient, which helps to prevent contamination and disease transmission. Gloves can be damaged during a surgical procedure, potentially harming both the surgeon and the patient. For the most part, glove perforation goes unnoticed by the wearer [1]. Being able to detect glove perforation would significantly aid the surgeon in determining when glove replacement is necessary. Perforations can significantly increase the risk of surgical site infection and expose the surgeon to blood-borne illnesses, such as HIV, hepatitis C, and hepatitis B [2,3].

Glove perforations occur commonly during surgical operations. Orthopaedic surgical procedures have the highest glove perforation rate compared to other types of surgery [4–6]. In orthopaedic surgery, the use of power equipment, handling sharp bones, and working in deep holes all contribute to the risk of glove perforation [4,6]. Various reports suggest that the causes of glove perforation include general wear after a given time period of use, hand dominance and, as already noted, the impact of certain surgical procedures [5].

One way to combat glove perforation is through 'double glove' use, whereby the wearer will put on at least two pairs of gloves. A glove perforation rate study revealed

that the total perforation rate between single and double glove sets is 15.2% and 14.4%, respectively [7]. It was shown that double gloving yielded 141 perforations from 512 glove sets, whereby the number of inner gloves perforated as a consequence of puncture from the outer to the inner gloves was 1.17%. Thus, even if the outer gloves were perforated, double gloving provided 98.83% protection. Another study reported that using double gloves for surgery resulted in an inner glove perforation rate of 3.7% [8]. The double gloving approach to manage glove perforation has been shown to be effective and provide greater than 90% protection for both the patient and the surgeon. However, given the potential life-threatening consequences of torn gloves, this rate is still far from ideal and wearing two pairs of gloves can compromise tactile sensitivity, manual dexterity and two-point discrimination [9]. Avoiding glove perforation is perhaps impossible; consequently, it becomes necessary to provide a fail-safe so that when tears do inevitably occur they can be quickly identified and remedied. According to Ashton et al., identifying certain surgical processes or scenarios when glove contamination is high may assist the surgeon in determining whether a glove change is required [10]. Needless to say, surgeons work under extreme pressure and stressful conditions; thus, checking for glove defects whilst undergoing a surgical procedure is a concern that we envision can be removed. Rather than doctors being aware of certain surgical scenarios that may result in damaged gloves, we suggest that wearing an integrated glove-damage detection device can provide rapid feedback in the event of a tear, allowing swift remediation, significantly reducing the risk of infection. Hence, in this work, we have sought to design and develop a novel glove topology that can provide the wearer with instant visual feedback when perforation occurs.

Curcumin is a polyphenolic compound mainly found in turmeric (*Curcuma longa* L.). It has received increasing interest from numerous studies owing to its health benefits such as anti-inflammatory, anti-diabetic, anti-microbial and anti-oxidant properties [3], as well as being relatively safe for human use [11]. Curcumin has good optical properties because of the symmetric structure of delocalized π electrons. Two benzene rings at the terminal of the curcumin molecule are joined by a seven-carbon heptadiene chain comprising a β -unsaturated β -diketone structure that shows keto-enol tautomerism (Figure 1), resulting in an extensive large delocalized-conjugated system and rigid planar structure [11]. Because of its optical properties as a fluorescent polyphenol, curcumin can be employed as a sensing material for the detection of chemicals [12]. Curcumin-based fluorescent probes can solve the lack of organic fluorescent dyes, for example, low quantum yield, and poor photostability [13,14]. Furthermore, since curcumin possesses multifunctional based fluorescence probes with high sensitivity, selectivity, and stability, much research has been published on chemosensor [15–24] and biosensor [25–32] applications of curcumin [12]. Thus, a strong body of foundational knowledge relating to the use of this compound is readily available.

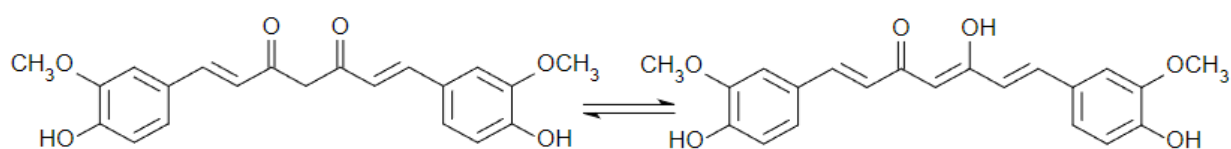


Figure 1. The keto-enol tautomeric structure of curcumin.

In previous work, we have shown how NRL can be modified to improve its antimicrobial properties for potential use as a stethoscope diaphragm cover [33]. In this research, we focus on the design and development of a novel torn-glove fluorescence-based sensor by filling curcumin in NRL compounding. The fluorescence of the curcumin coating/dipping layer beneath NRL helps to indicate the appearance of tearing or perforation under UV light. UV lights are commonly used in hospitals and especially in the operating theatre for surface and air disinfection purposes. Jerry et al. reported that using UV lights in the operating theatre during total joint replacement surgery appears to be an effective technique to reduce infection risk when necessary safety precautions are performed [34].

UV light in the operating room is equally effective as laminar airflow in reducing the number of bacteria and infection rates in the operating room by destroying bacteria [35]. Conceivably, the production of a torn glove fluorescence-based sensor will help to detect any perforation damage to the glove under the illumination of UV light.

2. Materials and Methods

2.1. Materials and Instrumentation

Curcumin (Cur) dispersion was extracted from turmeric by ethanol extraction and centrifuged for 15 min at 6000 rpm. Ethanol (98–100%) was acquired from Merck. The compounded NRL was purchased from Getahindus Sdn. Bhd., Malaysia. The total solid content (TSC) of compounded NRL is 60.8% and was diluted to 44% by adding distilled water. The latex compounded total solid content (TSC, %) was determined according to ISO 2004:2005 (E) Fifth Edition 1 September 2010.

2.2. Preparation of NRL Filled with Curcumin (NRL-Cur Mixture)

In total, 6.7% (TSC) of curcumin dispersion was mixed with NRL at 0.5 phr. Distilled water was added to the NRL-Cur compounding for dilution to TSC of 26%. The mixture was then stirred for 2 h and left for latex maturation at room temperature for 24 h before being used.

2.3. Preparation of Double Coating Films (LC)

The double coating films, which are NRL as the first dipping and NRL-Cur mixture as the second dipping (LC), were prepared firstly by the coagulant dipping process. At first, a cleaned and dried porcelain former was dipped into a slurry coagulant of 10% calcium nitrate solution for 10 s and dried in an oven at 70 °C for 10 min. Then, the former was dipped into the NRL compound based on the dwell time mentioned in Table 1, followed by drying in the oven at 100 °C for 15 min. The dried NRL films were taken out from the oven for ~5 min until the film temperature reached 55–60 °C. Then, the former continues to be dipped in NRL-Cur mixture for a few seconds (as dwell time stated in Table 1) and dried in the oven for 15 min at 100 °C before stripping out from the former using calcium carbonate powder. The thickness of each test piece was measured using a thickness gauge (Mitutoyo Corp., Kawasaki, Japan, Model Mitutoyo 7301) and the average thickness was taken. The thickness of film preparation needs to be controlled in the range of 0.20–0.26 mm by varying the dipping dwell time.

Table 1. Dwell time of LC film samples and their thickness.

Samples	Dwell Time		Thickness (mm)
	NRL (44%)	NRL-Cur (26%)	MEAN (\pm SD)
LC1	10_10	5_5	0.22 (2.78×10^{-17})
LC2	10_10	5	0.21 (2.78×10^{-17})
LC3	10_5_10	5_5	0.24 (4.90×10^{-3})
LC4	10_5_10	5	0.23 (4.00×10^{-3})
LC5	15_15	5_5	0.24 (8.94×10^{-3})
LC6	15_15	5	0.23 (4.90×10^{-3})
LC7	15_5_15	5_5	0.26 (4.90×10^3)
LC8	15_5_15	5	0.25 (4.30×10^3)
LC9	15_15	10_5_10	0.26 (0.00)
LC10	15_15	10_10	0.25 (4.71×10^{-3})
L	10_10		0.15 (0.00)

L = NRL film, LC = double coating of NRL with NRL-Cur film, Dwell time = 10_10 means 10 s dip in, and 10 s take out, while 10_5_10 means 10 s dip in, 5 s hold and 10 s take out, (\pm SD) = Standard Deviation.

2.4. Post-Processing of LC Film

Three optimum samples of LC films were chosen for post-processing. In the post-processing stage, the impact of various leaching situations on mechanical properties and fluorescence of LC films were investigated. The leaching procedure included wet-gel leaching, dry-gel leaching, and a combination of wet and dry gel leaching. This process is essential for producing NRL gloves because it removes soluble protein and excess chemicals [36]. For wet-gel leaching condition, after second dipping of NRL-Cur, the dipping plates were allowed to cool for 10 min before being wet-gel leached in distilled water at 70 °C for 1 min. Then, LC films were vulcanized and stripped. For dry-gel leaching, the LC films were stripped from the plates after vulcanization, and then they were soaked in distilled water for 1 h at room temperature. While, for a combination of wet and dry leaching, before vulcanization, the LC films were leached in distilled water at 70 °C for 1 min. Then, after stripping, the LC films were re-leached in distilled water for 1 h at room temperature. Figure 2 illustrates the leaching process for the optimised LC film. Leaching is a critical technique in the production of medical gloves because it is the most practical way to reduce undesired elements in rubber gloves while maintaining a clean product. Effective elimination of extractable proteins (which cause Type 1 allergy) and residual chemicals (which cause Type IV skin irritation) requires a mix of wet gel and dry leaching methods [37]. The mechanical properties and fluorescence of the LC films were determined for each leaching condition.

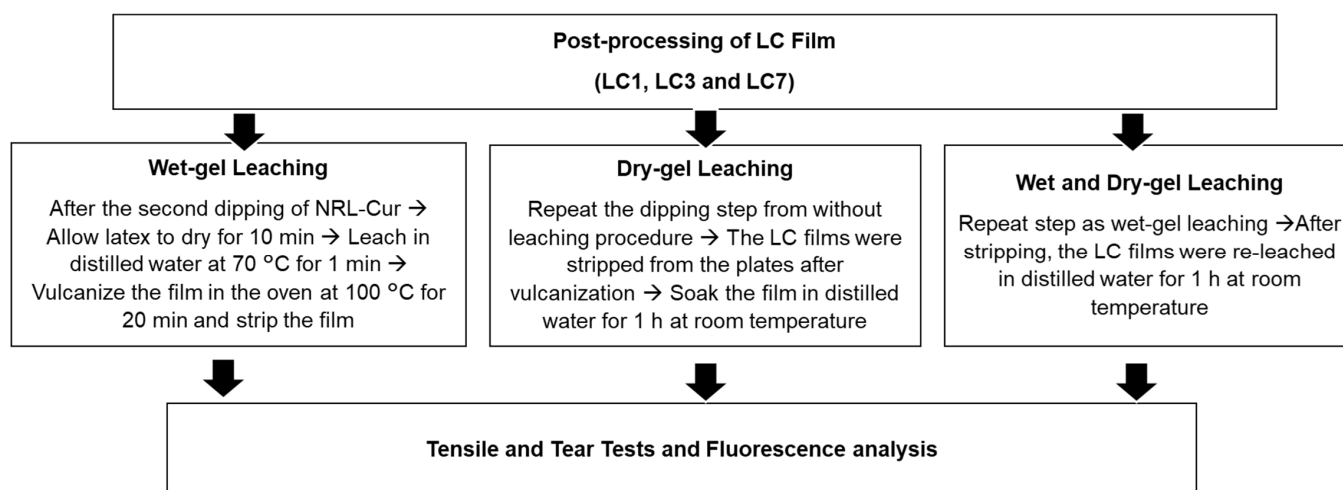


Figure 2. Flow chart of optimised LC films post-processing process.

2.5. Characterization of Mechanical Properties

Dumbbell shaped test pieces were cut from the LC films. The tensile test was done following the ASTM D416 standard using a computerized tensile tester machine (Instron Corp., Norwood, MA, USA, Model Instron 5564). The crosshead speed of the Instron machine was set at 500 mm/min until the test pieces failed. The values of tensile properties were the average of 5 measurements. A tear test was conducted according to the ASTM D624 standard. The LC films were cut into angle test specimens in the dipping direction. The tear test was carried out using an Instron machine with a crosshead speed of 500 mm/min \pm 50 mm/min until the test pieces failed. The tear strength was obtained, and the average of 5 readings was recorded.

2.6. Fluorescence Spectroscopy of LC Films

Fluorescence analysis of the LC films was measured by using a Fluorescence Spectrometer (PerkinElmer Inc., Waltham, MA, USA, Model PerkinElmer LS 55 Fluorescence Spectrometer). The excitation wavelength was set at 380 nm, and the fluorescence emission spectrum was scanned from 400 to 600 nm with a scan rate of 50 nm s⁻¹. The LC

films were cut into a circle (~2 cm diameter) and placed in the solid compartment of the fluorescence spectrometer. Four v-shaped lines were cut (~1.40 cm to each line) into the films so as to simulate a puncture or tear, as illustrated in Figure 3. The cuts in the NRL film are clearly visible when examined under UV light (380 nm) and this is also evident in the corresponding fluorescence emission spectra results (see Section 3.2 and supporting information, Figures S1–S10).



Figure 3. Photograph of LC films for solid sample fluorescence analysis (a) film under visible light, (b) film under UV light.

2.7. Characterization of LC Films

Fourier Transformed Infrared Spectroscopy (FTIR) spectra of the samples were recorded using a FTIR Spectrometer (Bruker Optics, MA, USA, Model Alpha) in transmission mode with the wavenumber ranging from 4000 to 500 cm^{-1} for sample functional groups characterization.

2.8. Thermogravimetric Analysis

Thermogravimetric analysis (TGA) was observed using a TGA analyzer (Perkin Elmer, MA, USA, Model Pyris 6) with a temperature range from 30 to 600 $^{\circ}\text{C}$ at a heating rate of 20 $^{\circ}\text{C}/\text{min}$ under a nitrogen atmosphere at a flow rate of 10 mL/min. The weight loss was calculated from the initial and final weight of the thermograms obtained as follows (Equation (1)):

$$\text{Weight loss (\%)} = \frac{(\text{Initial weight} - \text{Final weight})}{\text{Initial weight}} \times 100 \quad (1)$$

3. Results and Discussions

3.1. Mechanical Properties of the LC Films

Table 2 shows LC films' tensile and tear strengths with a different dwell time of NRL and LC mixture dipping. All the LC films showed better tensile and tear strength than the control sample of NRL alone. The tensile strength of the LC films for "5_5" dwell time of curcumin NRL-Cur mixture dipping (LC1, LC3, LC5, LC7) showed better strength than 5 s dwell time films (LC2, LC4, LC6, LC8). In contrast, the tear strength of LC2, LC4, LC6, and LC8 (5 s dwell time) films was better than that of LC1, LC3, LC5, and LC7 films ("5_5" dwell time). It showed that increasing the dwell time of curcumin can provide better tensile strength but is still good in tear strength when compared to quick dipping (5 s, in and out) with the NRL-Cur mixture. This is due to the increase in film thickness caused by the accumulation of more latex on the former. As film formation time increases, more latex particles are able to settle and form continuous films, as evidenced by the increased crosslinking observed in cured NRL films [38]. However, the differences in tensile and tear strength for each LC film based on the "5_5" and "5" dwell times of LC mixture dipping are less than 1.75 MPa and 5.23 N/mm, respectively, which is a slight difference when compared to each similar dwell time of NRL dipping. The minimum allowable tensile strength values prescribed by ASTM standards range from 14 to 24 MPa, which depends on the glove type. Thus, the tensile strength data (Table 2) showed that the values are still within the specified range by ASTM standards.

Table 2. Mechanical properties of LC films before leaching.

Samples	Tensile Strength (MPa)	Tear Strength (N/mm)
	Mean (\pm SD)	Mean (\pm SD)
LC1	19.10 (0.96)	40.55 (10.15)
LC2	18.09 (0.69)	45.78 (9.49)
LC3	18.82 (1.76)	40.13 (7.87)
LC4	18.96 (1.76)	41.25 (8.60)
LC5	19.14 (0.73)	41.72 (1.66)
LC6	19.13 (1.47)	44.23 (9.51)
LC7	18.67 (0.81)	39.84 (4.23)
LC8	18.31 (0.77)	43.05 (14.41)
LC9	20.10 (0.45)	39.97 (13.08)
LC10	18.35 (0.55)	40.20 (3.19)
L	17.92 (0.17)	37.73 (6.14)

L = NRL film, LC = double coating of NRL with NRL-Cur film, (\pm SD) = Standard Deviation.

3.2. Fluorescence Effect of the Torn/Cut LC Films Based on Dwell Time of Dipping

Each of the films was fluorescence examined based on solid sample analysis. Based on the maximum fluorescence intensity in Figure 4 and the fluorescence spectrum of each film (Supporting Information, Figures S1–S10), it showed that the films' fluorescence intensity increased after tearing. Besides, dipping patterns' dwell time is also correlated to the fluorescence intensity of the torn/cut LC films. The longer the dwell duration of the LC mixture dipping, the higher the intensity of the fluorescence. For example, for the "5_5" dwell time LC mixture dipping for the torn sample, LC-T1 has higher fluorescence intensity than the "5" dwell time for film LC-T2, as illustrated in Figure 4. In this work, the dwell time for LC mixture dipping was confined to less than the dwell time of the first dipping of NRL. It is to conceal the appearance of the inner underneath film colour from the outside layer of NRL film since curcumin is obviously yellow with a strong yellowish-green fluorescence emission. Moreover, when compared based on the dwell time of NRL latex dipping, most of the LC films do not show much difference, especially with the similar dwell time of LC mixture dipping. As shown in Figure 4, torn films (T) of LC1, LC5, and LC9 had nearly identical maximum fluorescence intensities, similar to LC2, LC6, and LC10 films. However, torn films of LC3, LC4, LC7 and LC8 exhibited the largest fluorescence intensity. Based on this observation, the 5 secs dwell time of NRL dipping produced an increased fluorescence emission when torn than other dwell times. We suggest that this is due to the thicker NRL film layer, which yields an increased fluorescence effect when torn; other works have indicated a positive correlation between fluorescence intensity and film thickness, which we suspect is possibly the case here [39,40]. Even though "15_5_15" dwell time (LC7 and LC8) showed the highest emission intensity when torn, the thickness (0.25–0.26 mm) of the films were quite thick for glove production. However, it is still less than the maximum thickness of a surgical glove as specified by international standards [41].

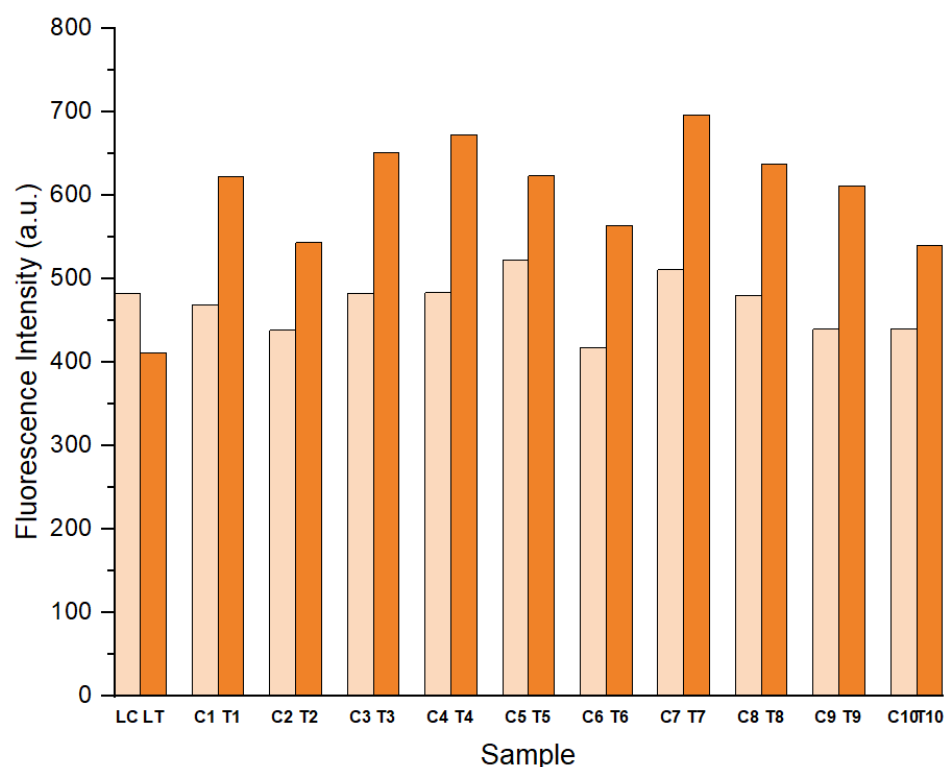


Figure 4. The maximum fluorescence intensity of each sample at emission wavelength 489 nm (LC = latex (without torn), LT = torn latex, C = control (i.e., without any tear), T = torn on the film).

3.3. Effect of Leaching Process on Mechanical Properties of the LC Films

Post-processing of the LC films is necessary to identify the effect of leaching. Therefore, the study was carried out to explore the optimum films (LC1, LC3 and LC7) on the mechanical properties of LC films and their fluorescence after the films were torn/cut. The films were chosen because they gave better results than other films when compared in mechanical tests, fluorescence intensity and the thickness of the film (which is within the recommended range for surgical glove thickness). The tensile and tear strengths of the LC films at different leaching conditions are shown in Table 3. Typically, leaching could increase the tensile strength of NR latex due to the elimination of water-soluble non-rubber substances, primarily proteins, and increase the efficient coalescence of rubber particles. As a result, leaching the proteins caused improved interaction between rubber molecules from nearby particles, resulting in a more coherent film [42]. Moreover, the excess calcium nitrate and water-soluble non-rubbers, such as additional compounding components, are also removed, which improves physical properties [43]. As shown in Table 3, the leaching LC films displayed greater tensile strength than the unleached NR latex film. The tear strength of the filled NR latex films increased after the leaching procedure. A combination of wet and dry gel leaching provided the best mechanical properties in tensile and tear strengths.

3.4. Effect of Leaching on Fluorescence Analysis of LC Films

The fluorescence emission intensity at 510 nm for LC1, LC3 and LC7 films after leaching are shown in Figure 5. It is demonstrated that wet leaching samples gave the highest fluorescence intensity, exhibiting a significant difference in intensity between the control and torn films. Moreover, each leaching sample gave higher intensity after being torn/cut than the control. Although, the dry leaching films show small gap difference in fluorescence intensity due to the leaching condition. The residue of curcumin dye from the curcumin-latex layer during dry leaching may affect the layer of NRL because the whole films were leaching after stripping; compared to wet leaching, only the curcumin-latex layer was leached in the water. After comparing leaching and without leaching, the fluorescence

intensity of leaching films is higher than without leaching. This comparison can also be observed visually in the images of the films under UV light in Table 4.

Table 3. Mechanical properties of LC1, LC3 and LC7 film post-processing (wet-gel leaching, dry-gel leaching, and wet and dry-gel leaching).

Leaching Conditions	LC1		LC3		LC7	
	Tensile (MPa)	Tear (N/mm)	Tensile (MPa)	Tear (N/mm)	Tensile (MPa)	Tear (N/mm)
Unleached	19.10	40.55	18.82	41.72	18.67	39.84
Wet	21.23	52.02	23.36	54.15	21.98	57.91
Dry	21.60	53.86	23.04	54.30	21.09	55.49
Wet + Dry	21.90	58.60	23.81	65.47	22.74	63.85

L = NRL film, LC = double coating of NRL with NRL-Cur film.

LC1DC = dry leaching of LC1 film without torn	LC3WT = wet leaching of LC3 film with torn
LC1DT = dry leaching of LC1 film with torn	LC3WDC = wet and dry leaching of LC3 film without torn
LC1WC = wet leaching of LC1 film without torn	LC3WDT = wet and dry leaching of LC3 film with torn
LC1WT = wet leaching of LC1 film with torn	LC7DC = dry leaching of LC7 film without torn
LC1WDC = wet and dry leaching of LC1 film without torn	LC7DT = dry leaching of LC7 film with torn
LC1WDT = wet and dry leaching of LC1 film with torn	LC7WC = wet leaching of LC7 film without torn
LC3DC = dry leaching of LC3 film without torn	LC7WT = wet leaching of LC7 film with torn
LC3DT = dry leaching of LC3 film with torn	LC7WDC = wet and dry leaching of LC7 film without torn
LC3WC = wet leaching of LC3 film without torn	LC7WDT = wet and dry leaching of LC7 film with torn

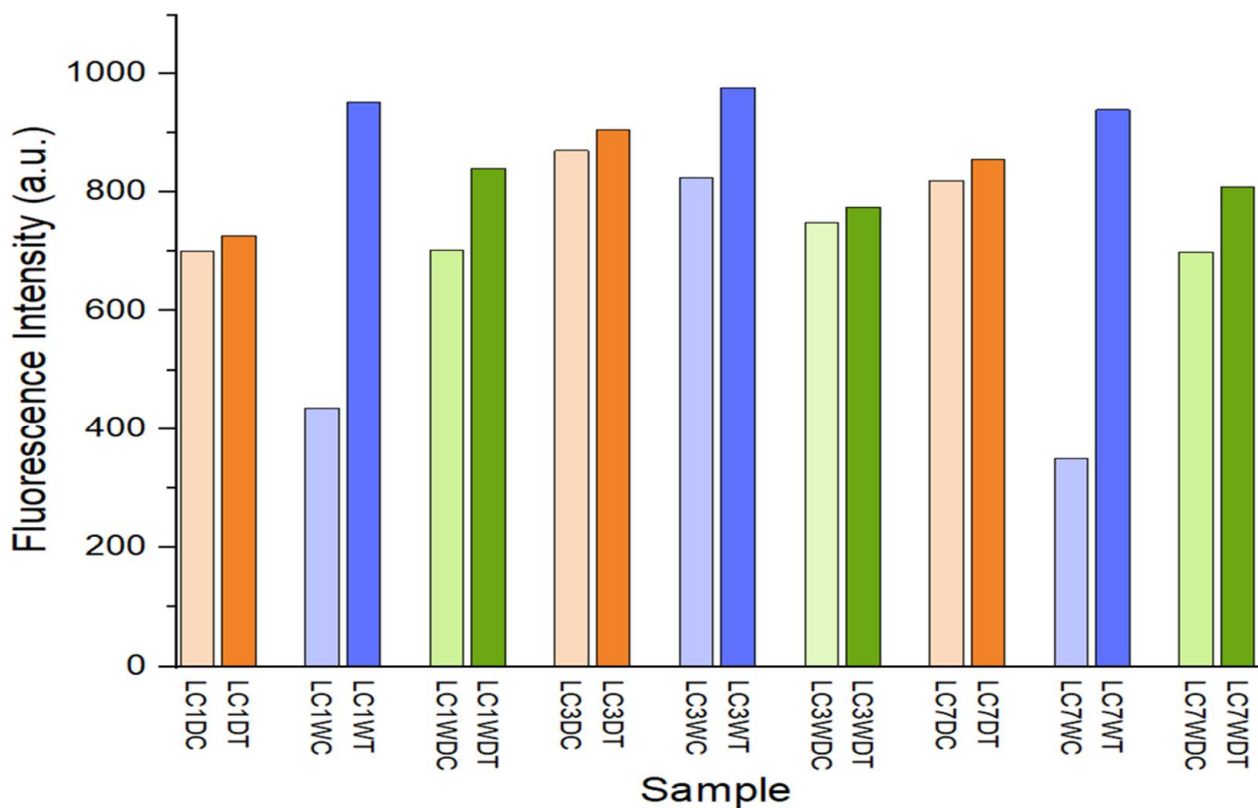














Figure 5. The fluorescence intensity of each sample after leaching at emission wavelength 510 nm.

Table 4. Images of LC1, LC3, and LC7 torn film before and after leaching.

LC Films	Without Leaching	Wet Leaching	Dry Leaching	Wet-Dry Leaching
LC1				
LC3				
LC7				

3.5. FTIR Study

Figure 6 illustrates the FTIR spectrum of NRL film, LC films, and curcumin. The characteristic peaks of *cis*-1,4-polyisoprene, at 2960 cm^{-1} , 2925 cm^{-1} , 2850 cm^{-1} (C–H stretching), 1661 cm^{-1} (C=C stretching), 1442 cm^{-1} (C–H bending of $-\text{CH}_2-$), 1374 cm^{-1} (C–H bending of $-\text{CH}_3$) and 841 cm^{-1} (C–H bending of C=C–H), characterize the NRL characteristics bands [44]. Curcumin showed its characteristic peaks at $3500\text{--}3000$ (phenolic O–H stretching vibration), 1626 cm^{-1} (aromatic moiety C=C stretching), 1585 cm^{-1} (benzene ring stretching vibrations), 1508 cm^{-1} (C=O and C=C vibrations), 1418 cm^{-1} (C–H bending vibrations), 1260 cm^{-1} (aromatic C–O stretching vibrations), and 1016 cm^{-1} (C–O–C stretching vibrations) [45]. Meanwhile, LC exhibited peaks at $3500\text{--}3000$ (phenolic O–H stretching vibration), 1641 cm^{-1} (aromatic moiety C=C stretching), 1578 cm^{-1} (benzene ring stretching vibrations) and 1535 cm^{-1} (C=O and C=C vibrations), while enol C–O peak was obtained at 1249 cm^{-1} , and C–O–C peak at 1012 cm^{-1} , which are the characteristic peaks of curcumin, indicating the existence of curcumin in the NRL films.

3.6. Thermal Properties by Thermogravimetric Analyzer (TGA)

Thermogravimetric analysis is a method for determining the mass change of a sample over time or at a specific temperature in a controlled environment. The measurement is generally used to ascertain the material's thermal and oxidative stabilities and its compositional properties. The weight losses due to heat degradation of NRL and LC films are depicted in Figure 7. The weight losses were calculated as a function of temperature. The first stage of deterioration of the NRL began at around $58\text{ }^\circ\text{C}$, whereas LC at $220\text{ }^\circ\text{C}$ since the absorbed water evaporated and ended at $450\text{ }^\circ\text{C}$ owing to the thermal decomposition of the rubber matrix. The mass loss peak found between 450 and $580\text{ }^\circ\text{C}$ was attributed to the rubber's heat breakdown of carbonaceous residues [46]. The temperature NRL and LC films at 5%, 50% and 75% weight loss, respectively, are shown in Table 5. As can be observed, the temperature of LC film steadily increased at 5% and 50% weight loss than in NRL. However, then, the temperature decreased after 75% weight loss of LC film and yielded 100% total weight loss at $538\text{ }^\circ\text{C}$. It showed that the thermal stability has reduced

due to the presence of curcumin, a higher unsaturated compound with more double bonds than NRL, which caused slightly lower oxidative stability.

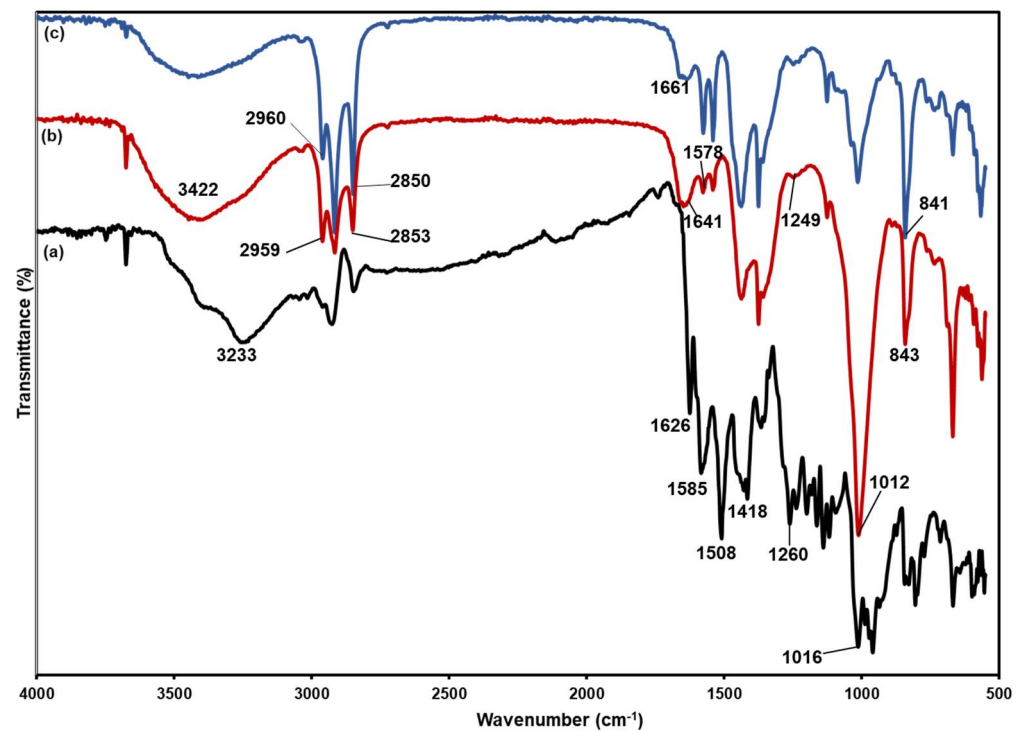


Figure 6. FTIR spectrum of (a) curcumin, (b) LC and (c) NRL.

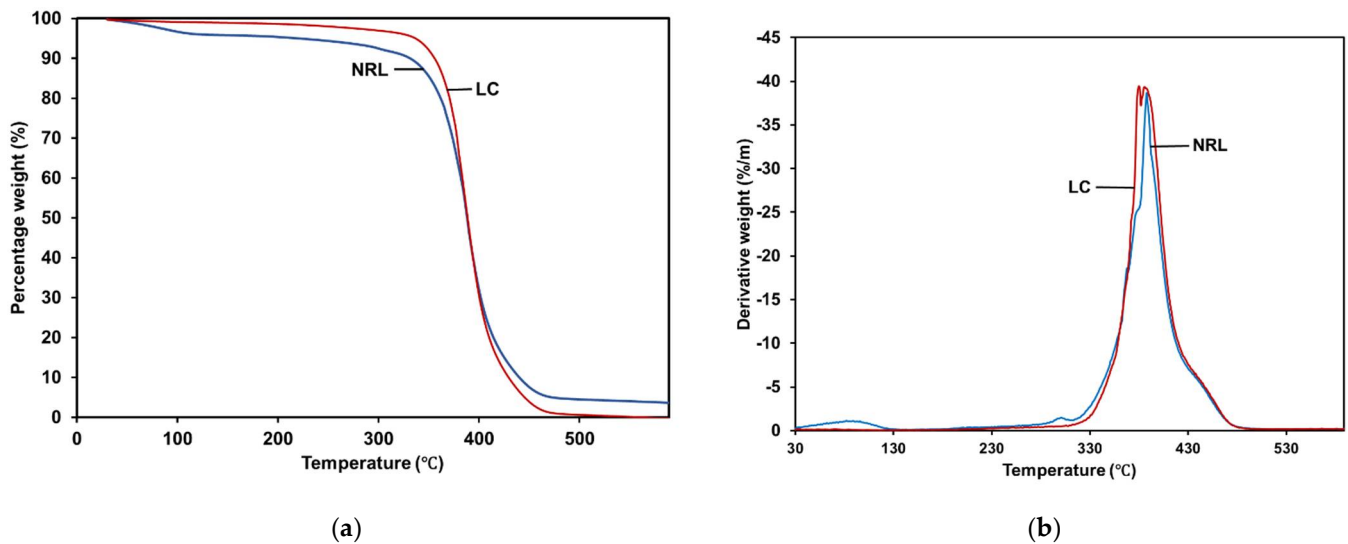


Figure 7. (a) TGA and (b) derivative thermogravimetry (DTG) curves of NRL and LC.

Table 5. The thermal stability comparison of NRL and LC.

Type of Film	T _{5%} (°C)	T _{50%} (°C)	T _{75%} (°C)	Total Weight Loss (%)
NRL	211.92	387.92	405.92	96.329
LC	336.92	388.92	403.92	100

4. Conclusions

In this research article, we presented a novel wearable glove design that combines latex and curcumin natural dyes for detecting torn or punctured gloves. We have demonstrated that the latex-curcumin (LC) layer can provide a clear optical signal to indicate that the material has torn. Further, our glove is made from low-cost materials, is remarkably simple to fabricate using curcumin extracted from turmeric and is safe to wear. The LC films' mechanical properties were comparable to the control sample's tensile strength but with higher tear strength; although, this was not the case for all films. The increasing dwell time of the dipping process does not significantly affect tensile or tear strength. However, after post-processing, the mechanical characteristics of LC films showed better tensile and tear strengths than those without leaching. As a result, double-layer LC beneath NRL films provides good structural stability for a fluorescence-based glove puncture detection system. Due to the high mechanical qualities and a high emission fluorescence intensity when ripped, LC3 and LC7 films offer optimal performance for LC glove production. This verification work has shown the potential benefit of LC as a wearable glove for in situ torn glove detection. In the future, it is hoped that the LC glove can be verified in a clinical study to demonstrate surgical glove tear detection in vivo in a suitable operating environment with appropriate lighting conditions available. Moreover, surgeons require maximum feeling and dexterity to perform the surgery successfully, and the gloves used should significantly prevent infection risk but not at the expense of surgical performance. Our novel integrated glove tearing sensor improves the mechanical strength of the NRL glove using compounds that are generally thought to be safe. Furthermore, it does so in a manner that allows tears to be readily detected in situ by the surgical team, whilst only requiring a single glove to be worn, which should enable the surgeon to perform their duties without compromising tactile sensitivity and manual dexterity.

Supplementary Materials: The following supporting information can be downloaded at: <https://www.mdpi.com/article/10.3390/polym14153048/s1>, Figures S1–S10. Fluorescence emission spectrum from LC1–LC10 samples. (inset: NRL-Cur films under UV lamp at 380 nm).

Author Contributions: Conceptualization, A.A.R. and S.M.; designing the experiments, writing, editing, and analyzing data, N.M.S.; designing the experiments, analyzing data, and writing, N.S.D.; writing, review, and editing, A.A.R. and S.M.; supervision and project administration, A.A.R. All authors have read and agreed to the published version of the manuscript.

Funding: This research was funded by the Universiti Sains Malaysia from Research University Grant Scheme (grant no: 1001/PBAHAN/8014155).

Data Availability Statement: All the actual data are presented in the manuscript.

Acknowledgments: The authors would like to thank the Malaysia Ministry of Higher Education for financial assistance and the School of Materials and Mineral Resources Engineering, Universiti Sains Malaysia for support and facilities for this research project.

Conflicts of Interest: The authors declare no conflict of interest.

References

1. Chan, K.Y.; Singh, V.A.; Oun, B.H.; To, B.H.S. The rate of glove perforations in orthopaedic procedures: Single versus double gloving. A prospective study. *Med. J. Malays.* **2006**, *61* (Suppl. B), 3–7.
2. Osman, M.O.; Jensen, S.L. Surgical Gloves: Current Problems. *World J. Surg.* **1999**, *23*, 630–637. [[CrossRef](#)] [[PubMed](#)]
3. Dodds, R.D.A.; Guy, P.J.; Peacock, A.M.; Duffy, S.R.; Barker, S.G.E.; Thomas, M.H. Surgical glove perforation. *Br. J. Surg.* **2005**, *75*, 966–968. [[CrossRef](#)] [[PubMed](#)]
4. Han, C.D.; Kim, J.; Moon, S.H.; Lee, B.H.; Kwon, H.M.; Park, K.K. A Randomized Prospective Study of Glove Perforation in Orthopaedic Surgery: Is a Thick Glove More Effective? *J. Arthroplast.* **2013**, *28*, 1878–1881. [[CrossRef](#)]
5. Tanner, J. Surgical Gloves: Perforation and Protection. *J. Perioper. Pract.* **2006**, *16*, 148–152. [[CrossRef](#)]
6. Yinusa, W.; Li, Y.H.; Ho, W.Y.; Leong, J.C.Y.; Chow, W. Glove punctures in orthopaedic surgery. *Int. Orthop.* **2004**, *28*, 36–39. [[CrossRef](#)]

7. Makama, J.G.; Okeme, I.M.; Makama, E.J.; Ameh, E.A. Glove Perforation Rate in Surgery: A Randomized, Controlled Study To Evaluate the Efficacy of Double Gloving. *Surg. Infect.* **2016**, *17*, 436–442. [[CrossRef](#)] [[PubMed](#)]
8. Gordon, A.M.; Hudson, P.W.; Bowman, J.R.; Watson, S.L.; Leddy, L.R.; Khoury, J.G.; Patt, J.C.; Tubb, C.C.; Ames, S.E.; McGwin, G.; et al. Workplace Hazards in Orthopaedic Surgery Training: A Nationwide Resident Survey Involving Sharps-related Injuries. *J. Am. Acad. Orthop. Surg.* **2022**, *30*, 428–436. [[CrossRef](#)]
9. Germaine, R.L.S.; Hanson, J.; de Gara, C.J. Double gloving and practice attitudes among surgeons. *Am. J. Surg.* **2003**, *185*, 141–145. [[CrossRef](#)]
10. Goldman, A.H.; Haug, E.; Owen, J.R.; Wayne, J.S.; Golladay, G.J. High Risk of Surgical Glove Perforation From Surgical Rotatory Instruments. *Clin. Orthop. Relat. Res.* **2016**, *474*, 2513–2517. [[CrossRef](#)]
11. Liu, Y.; Zhang, C.; Pan, H.; Li, L.; Yu, Y.; Liu, B. An insight into the in vivo imaging potential of curcumin analogues as fluorescence probes. *Asian J. Pharm. Sci.* **2021**, *16*, 419–431. [[CrossRef](#)] [[PubMed](#)]
12. Khorasani, M.Y.; Langari, H.; Sany, S.B.T.; Rezayi, M.; Sahebkar, A. The role of curcumin and its derivatives in sensory applications. *Mater. Sci. Eng. C* **2019**, *103*, 109792. [[CrossRef](#)] [[PubMed](#)]
13. Zakaria, H.; El Kurdi, R.; Patra, D. A Novel Study on the Self-Assembly Behavior of Poly(lactic-co-glycolic acid) Polymer Probed by Curcumin Fluorescence. *ACS Omega* **2022**, *7*, 9551–9558. [[CrossRef](#)]
14. Sirawatcharin, S.; Saithongdee, A.; Chaicham, A.; Tomapatanaget, B.; Imyim, A.; Praphairaksit, N. Naked-eye and Colorimetric Detection of Arsenic(III) Using Difluoroboron-curcumin in Aqueous and Resin Bead Support Systems. *Anal. Sci.* **2014**, *30*, 1129–1134. [[CrossRef](#)]
15. Bhopate, D.P.; Mahajan, P.G.; Garadkar, K.M.; Kolekar, G.B.; Patil, S.R. A highly selective and sensitive single click novel fluorescent off-on sensor for copper and sulfide ions detection directly in aqueous solution using curcumin nanoparticles. *New J. Chem.* **2015**, *39*, 7086–7096. [[CrossRef](#)]
16. Xu, G.; Wang, J.; Si, G.; Wang, M.; Xue, X.; Wu, B.; Zhou, S. A novel highly selective chemosensor based on curcumin for detection of Cu²⁺ and its application for bioimaging. *Sens. Actuators B Chem.* **2016**, *230*, 684–689. [[CrossRef](#)]
17. Ponnuvel, K.; Santhiya, K.; Padmini, V. Curcumin based chemosensor for selective detection of fluoride and cyanide anions in aqueous media. *Photochem. Photobiol. Sci.* **2016**, *15*, 1536–1543. [[CrossRef](#)]
18. Liu, Y.; Ouyang, Q.; Li, H.; Zhang, Z.; Chen, Q. Development of an Inner Filter Effects-Based Upconversion Nanoparticles–Curcumin Nanosystem for the Sensitive Sensing of Fluoride Ion. *ACS Appl. Mater. Interfaces* **2017**, *9*, 18314–18321. [[CrossRef](#)]
19. Park, S.; Lee, S.-Y. Significant enhancement of curcumin photoluminescence by a photosensitizing organogel: An optical sensor for pyrrole detection. *Sens. Actuators B Chem.* **2015**, *220*, 318–325. [[CrossRef](#)]
20. Ashraf, P.M.; Lalitha, K.; Edwin, L. Synthesis of polyaniline hybrid composite: A new and efficient sensor for the detection of total volatile basic nitrogen molecules. *Sens. Actuators B Chem.* **2015**, *208*, 369–378. [[CrossRef](#)]
21. Ramamoorthy, J.; Sathya, V.; Lavanya, R.; Padmini, V. Highly selective and sensitive response of curcumin thioether derivative for the detection of hypochlorous acid by fluorimetric method. *J. Iran. Chem. Soc.* **2022**, *19*, 3327–3335. [[CrossRef](#)]
22. Devasena, T.; Balasubramanian, N.; Muninathan, N.; Baskaran, K.; John, S.T. Curcumin Is an Iconic Ligand for Detecting Environmental Pollutants. *Bioinorg. Chem. Appl.* **2022**, *2022*, 9248988. [[CrossRef](#)]
23. Chandran, N.; Janardhanan, P.; Bayal, M.; Pilankatta, R.; Nair, S.S. Development of a paper printed colorimetric sensor based on Cu-Curcumin nanoparticles for evolving point-of-care clinical diagnosis of sodium. *Sci. Rep.* **2022**, *12*, 1–15. [[CrossRef](#)]
24. Geng, F.; Wang, Y.; Qu, P.; Zhang, Y.; Dong, H.; Xu, M. Naked-eye detection of Cys using simple molecular systems of curcumin and Hg²⁺. *Anal. Methods* **2013**, *5*, 3965–3969. [[CrossRef](#)]
25. Patil, R.; Gangalum, P.R.; Wagner, S.; Portilla-Arias, J.; Ding, H.; Rekechenetskiy, A.; Konda, B.; Inoue, S.; Black, K.L.; Ljubimova, J.Y.; et al. Curcumin Targeted, Polymalic Acid-Based MRI Contrast Agent for the Detection of A β Plaques in Alzheimer’s Disease. *Macromol. Biosci.* **2015**, *15*, 1212–1217. [[CrossRef](#)]
26. Alipour, E.; Shahabi, H.; Mahmoudi-Badiki, T. Introducing curcumin as an electrochemical DNA hybridization indicator and its application for detection of human interleukin-2 gene. *J. Solid State Electrochem.* **2016**, *20*, 1645–1653. [[CrossRef](#)]
27. Ojani, R.; Raoof, J.-B.; Zamani, S. A novel voltammetric sensor for amoxicillin based on nickel–curcumin complex modified carbon paste electrode. *Bioelectrochemistry* **2012**, *85*, 44–49. [[CrossRef](#)] [[PubMed](#)]
28. Pourreza, N.; Golmohammadi, H. Hemoglobin detection using curcumin nanoparticles as a colorimetric chemosensor. *RSC Adv.* **2015**, *5*, 1712–1717. [[CrossRef](#)]
29. Estephan, M.; El Kurdi, R.; Patra, D. Curcumin-embedded DBPC liposomes coated with chitosan layer as a fluorescence nanosensor for the selective detection of ribonucleic acid. *Luminescence* **2022**, *37*, 422–430. [[CrossRef](#)]
30. Erna, K.H.; Felicia, W.X.L.; Rovina, K.; Vonnice, J.M.; Huda, N. Development of curcumin/rice starch films for sensitive detection of hypoxanthine in chicken and fish meat. *Carbohydr. Polym. Technol. Appl.* **2022**, *3*, 100189. [[CrossRef](#)]
31. Dai, H.; Huang, Z.; Liu, X.; Bi, J.; Shu, Z.; Xiao, A.; Wang, J. Colorimetric ELISA based on urease catalysis curcumin as a ratiometric indicator for the sensitive determination of aflatoxin B1 in grain products. *Talanta* **2022**, *246*, 123495. [[CrossRef](#)] [[PubMed](#)]
32. Sarih, N.M.; Gwee, K.; Maher, S.; Rashid, A.A. Natural Rubber (NR) Latex Films with Antimicrobial Properties for Stethoscope Diaphragm Covers. *Materials* **2022**, *15*, 3433. [[CrossRef](#)] [[PubMed](#)]
33. Ritter, M.A.; Olberding, E.M.; Malinzak, R.A. Ultraviolet Lighting During Orthopaedic Surgery and the Rate of Infection. *JBSJ* **2007**, *89*, 1935–1940. [[CrossRef](#)]
34. Ritter, M.A. Operating Room Environment. *Clin. Orthop. Relat. Res.* **1999**, *369*, 103–109. [[CrossRef](#)] [[PubMed](#)]

35. Yew, G.Y.; Tham, T.C.; Law, C.L.; Chu, D.-T.; Ogino, C.; Show, P.L. Emerging crosslinking techniques for glove manufacturers with improved nitrile glove properties and reduced allergic risks. *Mater. Today Commun.* **2019**, *19*, 39–50. [[CrossRef](#)]
36. Huda, N.; Mohd, A.-H. Leaching A Critical Factor in processing of rubber examination gloves. *Malays. Rubber Technol. Dev.* **2014**, *1*, 16–21.
37. Ab Rahman, M.F.; Rusli, A.; Kuwn, M.T.; Azura, A.R. Effect of Latex Compound Dwell Time for the Production of Prototyped Biodegradable Natural Rubber Latex Gloves. *IOP Conf. Ser. Mater. Sci. Eng.* **2019**, *548*, 012017. [[CrossRef](#)]
38. Myant, C.; Reddyhoff, T.; Spikes, H. Laser-induced fluorescence for film thickness mapping in pure sliding lubricated, compliant, contacts. *Tribol. Int.* **2010**, *43*, 1960–1969. [[CrossRef](#)]
39. Goldys, E.M.; Drozdowicz-Tomsia, K.; Xie, F.; Shtoyko, T.; Matveeva, E.; Gryczynski, I.; Gryczynski, Z. Fluorescence Amplification by Electrochemically Deposited Silver Nanowires with Fractal Architecture. *J. Am. Chem. Soc.* **2007**, *129*, 12117–12122. [[CrossRef](#)]
40. Chirinos, H.D.; Guedes, S.M.L. The manufacture of gloves using RVNRL: Parameters of the coagulant dipping process. *Braz. J. Chem. Eng.* **1998**, *15*, 334–342. [[CrossRef](#)]
41. Ramli, R.; Jaapar, J.; Singh, M.S.J.; Yatim, A.H.M. Physical Properties and Fatigue Lifecycles of Natural Rubber Latex Gloves. *Adv. Environ. Biol.* **2014**, *8*, 2714–2722.
42. Mathew, S.; Varghese, S. Extractable Proteins in Latex Products: Effect of Vulcanization Methods and Leaching. *Rubber Sci.* **2019**, *31*, 249–258.
43. Wei, F.; Yu, H.; Zeng, Z.; Liu, H.; Wang, Q.; Wang, J.; Li, S. Preparation and structural characterization of hydroxyethyl methacrylate grafted natural rubber latex. *Polímeros* **2014**, *24*, 283–290. [[CrossRef](#)]
44. Chen, X.; Zou, L.-Q.; Niu, J.; Liu, W.; Peng, S.-F.; Liu, C.-M. The Stability, Sustained Release and Cellular Antioxidant Activity of Curcumin Nanoliposomes. *Molecules* **2015**, *20*, 14293–14311. [[CrossRef](#)] [[PubMed](#)]
45. Nabil, H.; Ismail, H.; Azura, A. Recycled Polyethylene Terephthalate Filled Natural Rubber Compounds: Effects of Filler Loading and Types of Matrix. *J. Elastomers Plast.* **2011**, *43*, 429–449. [[CrossRef](#)]
46. Chaichua, B.; Prasassarakich, P.; Poompradub, S. In situ silica reinforcement of natural rubber by sol–gel process via rubber solution. *J. Sol-Gel Sci. Technol.* **2009**, *52*, 219–227. [[CrossRef](#)]